Figure captions

Figure 1S: ORTEP plot of the dicationic unit **a** = $[Ni_2(C_{42}H_{42}N_6O_4S_2)]^{2+}$ showing the second independent entitiy $\mathbf{a_2}$ with atom labels and numbering scheme. Hydrogens are omitted for clarity. Ellipsoids are drawn at the 35% probability level.

Figure 2S: Temperature dependence of the product of the temperature and the molar susceptibility for $\mathbf{a(BPh_4)_2}$ at 0.5 T (Δ), 1 T (∇), 2.5 T (◊), and 5 T (O) magnetic field with the best least-squares fits (solid line).

Figure 3S: ^{1}H magnitude COSY spectrum (A) and downfield portion of the ^{1}H NMR spectrum (B) of $\mathbf{b(PF_6)_2}$ in CD_2Cl_2 at 293 K. Data are acquired and processed identically to the COSY experiment presented in Figure 5 of the manuscript. Pyridyl and thiophenolic spin-systems are shown. Part (C) emphasizes the spin-system of the thiophenolic aromatic ring. Part (D) reproduces the ligand numbering scheme used for signal assignment.

Figure 4S: Portions of the magnitude COSY spectrum of $\mathbf{c(PF_6)_2}$ in CD_2Cl_2 at 293 K, describing (A) the pyridyl aromatic spin-systems and (B) the thiophenolic spin-systems. Py1 and Py1' stand for the *H1* non-methylated pyridyl ring; Py2 and Py2' stand for the methylated pyridyl ring.

Figure 5S: Observed relaxation rate *vs* reciprocal temperature for the resonance assigned to Py1-*H2* in the case of $\mathbf{a(BPh_4)_2}$ in CD_2Cl_2. The filled curve shows the result of a linear least-squares fit: Intercept = -0.38 ms^{-1}, slope = 204 $K.ms^{-1}$ and correlation coefficient = 0.993.

Table captions

Table 1S: Crystallographic experimental details for $\mathbf{a(BPh_4)_2}$.

Table 2S: NMR parameters and resonance assignment for the two binuclear Ni^{II} complexes $\mathbf{a(PF_6)_2}$ and $\mathbf{b(PF_6)_2}$ complexes in CD_2Cl_2 at 293 K. Results of chemical shift and relaxation rate temperature-dependence for complex $\mathbf{b(PF_6)_2}$ in CD_2Cl_2.

Table 3S: Resonance assignment, relaxation properties and temperature dependence of chemical shift values and relaxation rate, at 293 K, in the mixture of stereoisomers $\mathbf{c(PF_6)_2}$ in CD_2Cl_2.

Text captions

Syntheses and Physico-Chemical Characterizations.

Hyperfine shifts in nickel(II) dimers : Curie law deviations due to *D* and *J*.

Syntheses and Physico-Chemical Characterizations.

Ligands and intermediates syntheses.

7: 2-formaldoxime-6-methylpyridine (2.6 g, 19.12 mmol) was melted in 70 mL of dry MeOH and 10% Pd/C (270 mg) was added to the solution. The mixture was stirred at room temperature under hydrogen atmosphere. After 12 h, the mixture was filtered and the filtrate was evaporated to dryness. This procedure afforded 2 g of **7** (86% yield) as a pale yellow oil, which was used without any further purification.

Compounds **6** and **9** were prepared following the same procedure as described for compound **5**. For **6**, the pyridine-2-carboxaldehyde was substituted for 6-methylpyridine-2-carboxaldehyde; for **9**, the pyridine-2-carboxaldehyde was replaced for 6-methylpyridine-2-carboxaldehyde and secondary amine **4** by **8**. **6** was purified by chromatography on neutral alumina using ethyl acetate/cyclohexane (1/1 and 2/1, v/v) as eluant and was isolated as a pale yellow oil with 67% yield. **9** was purified by chromatography on neutral alumina using cyclohexane/ethyl acetate (2/1, v/v) as eluant. As the obtained product still contained impurities, a second run on neutral alumina, using cyclohexane/ethyl acetate (1:1, v/v) as eluant, afforded **9** as a pale yellow oil (43% yield).

Ligands and intermediates spectroscopic characterizations.

1: ^{1}H NMR (DMSO-d_6): δ 13.1 (s br, COO*H*), 7.98 (d, 1H, J = 3 Hz, HOOC-CAr-*oH*), 7.50 (m, 2H, Ar-*H*), 7.28 (m, 1H, RS-Ar-*oH*), 3.23 (t, 2H, J = 6.8 Hz, -SCH_2-), 2.80 (t, 2H, J = 6.8 Hz, -CH_2CN); ^{13}C NMR (DMSO-d_6): δ 167.6, 138.8, 132.6, 131.1, 128.8, 125.8, 124.6, 119.3, 26.7, 16.8; mass spectrum (EI), m/z = 207 $[M]^+$. Anal. Calcd for $C_{10}H_9NO_2S$: C, 57.96; H, 4.38; N, 6.76; S, 15.47. Found: C, 57.55; H, 4.42; N, 6.74; S, 15.29.

2: ^{1}H NMR ($CDCl_3$): δ 7.34 (m, 4H, Ar-*H*), 4.75 (s, 2H, -CH_2OH), 3.20 (s, 1H, -O*H*), 3.05 (t, 2H, J = 7.1 Hz, -SCH_2-), 2.53 (t, 2H, J = 7.1 Hz, -CH_2CN); ^{13}C NMR ($CDCl_3$): δ 142.5, 132.1, 131.4, 128.8, 128.4, 128.2, 118.0, 63.1, 30.2, 18.0; mass spectrum (EI), m/z = 193 $[M]^+$. Anal. Calcd for $C_{10}H_{11}NOS$: C, 62.15; H, 5.74; N, 7.25; S, 16.59. Found: C, 62.11; H, 5.75; N, 7.03; S, 16.57.

3: ^{1}H NMR ($CDCl_3$): δ 10.40 (s, 1H, -C*H*O), 7.88 (d, 1H, J = 2.8 Hz, Ar-*H*), 7.45 (m, 3H, Ar-*H*), 3.22 (t, 2H, J = 7.3 Hz, -SCH_2-), 2.69 (t, 2H, J = 7.3 Hz, -CH_2CN); ^{13}C NMR ($CDCl_3$): δ 191.1, 138.0, 134.5, 134.1, 132.3, 129.1, 126.7, 117.5, 28.9, 17.5; mass spectrum (EI), m/z = 191 $[M]^+$. Anal. Calcd for $C_{10}H_9NOS$: C, 62.28; H, 4.74; N, 7.32; S, 16.7 6. Found: C, 62.23; H, 4.76; N, 7.13; S, 16.97.

4: ^{1}H NMR ($CDCl_3$): δ 8.51 (d, 1H, J = 4.2 Hz, Py-*H1*), 7.62 (t, 1H, J = 7.6 Hz, Py-*H4*), 7.29 (m, 6H, Ar-*H*), 3.98 (s, 2H, NCH_2ArSR), 3.94 (s, 2H, NCH_2Py), 3.06 (t, 2H, J = 7.1 Hz, -SCH_2), 2.52 (t, 2H, J = 7.1 Hz, -CH_2CN), 2.32 (s br, N*H*); ^{13}C NMR ($CDCl_3$): δ 159.3, 148.9, 141.4, 136.1, 132.4, 131.1, 129.6, 129.4, 127.7, 122.0, 121.6, 117.8, 54.3, 51.3, 29.7, 17.8; mass spectrum (FAB), m/z = 281 $[M-2H]^+$.

6: ^{1}H NMR (300 MHz, $CDCl_3$): δ 8.51 (d, 1H, J = 5 Hz, Py-*H1*), 7.56 (m, 4H, Ar-*H*), 7.34 (m, 2H, Ar-*H*), 7.21 (m, 2H, Ar-*H*), 7.12 (t, 1H, J = 6 Hz, Ar-*H*), 6.98 (d, 1H, J = 7.5 Hz, Ar-*H*), 3.87 (s, 2H, NCH_2ArSR), 3.82 (s, 2H, NCH_2Py), 3.79 (s, 2H, CH_2PyCH_3), 3.09 (t, 2H, J = 7.0 Hz, -SCH_2-), 2.53 (m, 5H, -CH_2CN and CH_3); ^{13}C NMR (75.4 MHz, $CDCl_3$): δ 159.1,

158.4; 157.2, 148.6, 148.6, 140.3, 136.4, 136.1, 133.4, 130.3, 130.2, 127.7, 127.0, 123.0, 121.8, 121.2, 119.7, 117.9, 59.8, 59.8, 29.5, 24.2, 17.8.

7: ^{1}H NMR ($CDCl_3$): δ 7.52 (t, 1H, J = 7.6 Hz, Py-*H3*), 7.12 (d, 1H, J = 7.6 Hz, Py-*H4*), 7.00 (d, 1H, J = 7.6 Hz, Py-*H2*), 3.94 (s, 2H, NCH_2PyCH_3), 2.53 (s, 3H, $-CH_3$), 2.15 (s, br, $-NH_2$); ^{13}C NMR ($CDCl_3$): δ 158.9, 157.8, 136.7, 121.3, 119.0, 54.8, 24.3.

9: ^{1}H NMR ($CDCl_3$): δ 7.53 (m, 3H, Ar-*H*), 7.38 (d, 2H, J = 7.2 Hz, Ar-*H*), 7.23 (m, 2H, Ar-*H*), 7.31 (m, 1H, Ar-*H*), 6.99 (d, 2H, J = 10.2 Hz, Ar-*H*), 3.88 (s, 2H, NCH_2ArSR), 3.79 (s, 4H, NCH_2Py), 3.08 (t, 2H, J = 7.5 Hz, $-SCH_2-$), 2.51 (m, 8H, $-CH_2CN$ and $-CH_3$); ^{13}C NMR ($CDCl_3$): δ 158.7, 157.3, 140.6, 136.5, 133.4, 130.5, 130.3, 127.7, 127.2, 121.3, 119.7, 117.9, 60.1, 56.8, 29.7, 24.3, 17.9.

Dinuclear complexes a$(PF_6)_2$, b$(PF_6)_2$ and c$(PF_6)_2$.

a$(PF_6)_2$. The complex was prepared according to method-A procedure starting from **5** (218 mg, 0.58 mmol), $Ni(OAc)_2.4H_2O$ (0.58 mmol), and NH_4PF_6 (114 mg, 0.67 mmol) in methanol. The blue solution was concentrated and turned to green after one day. Slow evaporation afforded, after 10 days, a green microcrystalline precipitate which was isolated by filtration. Drying *in vacuo* gave 104 mg of **a$(PF_6)_2$** (30.6% yield), as a green powder. Anal. Calcd for $C_{42}H_{42}N_6O_4S_2Ni_2P_2F_{12}$: C, 43.25; H, 3.63; N, 7.21; S, 5.50; Ni, 10.07; F, 19.55. Found: C, 43.04; H, 3.64; N, 7.28; S, 6.51; Ni, 9.90; F, 18.46. Mass spectrum (FAB, matrix NBA), m/z = 1021 $[M - PF_6]^+$. IR (KBr, cm^{-1}): 2920, 1591(ν_{as}(COO)), 1432(ν_s(COO)), 1411, 844. UV-vis (acetone, λ_{max}, nm (ε, $M^{-1}.cm^{-1}$)) 332 (160), 550 (13), 940 (16).

Complexes **b$(PF_6)_2$** and **c$(PF_6)_2$** were respectively obtained with 33.5% and 31% yield using the same procedure. Mass spectra (FAB, matrix NBA): **b$(PF_6)_2$**, m/z = 1077 $[M + H - PF_6]^+$; **c$(PF_6)_2$**, m/z = 1047 $[M + H - PF_6]^+$.

Mononuclear complex m(PF_6).

m(PF_6). The complex was prepared according to the same procedure as **m(BPh_4)**, starting from 105 mg (0.28 mmol) of **5** with 70 mg of $Ni(OAc)_2.4H_2O$ (0.28 mmol) and 95 mg of NH_4PF_6 (0.58 mmol) in degassed methanol (5 mL). The blue-purple solution was cooled at -20 °C. After one week, the white precipitate was removed by filtration and the filtrate was concentrated by slow evaporation at 0 °C. After an additional week, a lavender-blue precipitate was formed. The resulting solid, isolated by filtration, was melted in acetone, and the solution was filtered. Evaporation of the solvent and drying *in vacuo* afforded 73.5 mg (27% yield) of **m(PF_6)** as a violet powder. This material was stable both in the solid state at room temperature and in acetone solution at -20 °C for months. Anal. Calcd for $C_{24}H_{24}N_4O_2SNiPF_6 \cdot 2MeOH$: C, 44.59; H, 4.61; N, 8.09; S, 4.58; Ni, 8.38; F, 16.28. Found: C, 44.44; H, 4.24; N, 8.23; S, 4.76; Ni, 7.98; F, 16.36. Mass spectrum (FAB, matrix NBA), m/z = 491 $[M - PF_6]^+$. IR (KBr, cm^{-1}): 3565, 2925, 2246, 1607.5, 1540 (ν_{as}(COO)), 1476, 1459, 1420 (ν_s(COO)), 1031, 843. UV-vis (acetone, λ_{max}, nm (ε, $M^{-1}.cm^{-1}$)): 408 (sh), 592 (6), 966 (4).

X-Ray data.

Figure 1S: ORTEP plot of the dicationic unit **a** = $[Ni_2(C_{42}H_{42}N_6O_4S_2)]^{2+}$ showing the second independent entitiy $\mathbf{a}_2$ with atom labels and numbering scheme. Hydrogens are omitted for clarity. Ellipsoids are drawn at the 35% probability level.

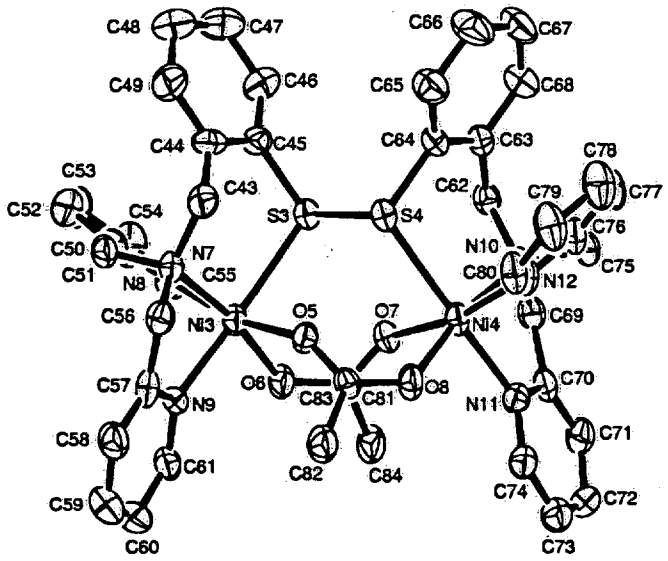

Table 1S: Crystallographic experimental details for $\mathbf{a}(BPh_4)_2$.

I. Crystal data

Formula: $[Ni_2S_2N_6C_{42}O_4H_{42}]\cdot 2[C_{24}BH_{20}]\cdot 1/2$solvate* Fw = 1638.48

Crystal System: triclinic	Space group: $P\bar{1}$
a = 18.128(7) Å α = 101.30(2)°	V = 8791(6) Å^3
b = 20.224(7) β = 104.07(2)	Z = 4
c = 26.221(9) γ = 102.37(3)	D_x = 1.238
Cell parameters from 24 reflections	θ = 10 - 12°
F(000) = 3452	
Linear absorption factor (λMoKα):	μ = 0.533 mm^{-1}
Morphology:	yellowish triclinic prism
Crystal dimensions	0.22, 0.21, 0.19 mm

II. Intensity measurements

Temperature:	293 K
Diffractometer:	Enraf Nonius CAD-4
Monochromator:	graphite
Radiation:	λMoKα = 0.07107 Å
Scan mode:	ω
Scan width:	1.20°
Data collection limits:	$2.1 \le \theta \le 22.1$
Measured reflections: 17557	independent reflections: 16972

Table 1S (continued) :

III. Structure determination and refinement

Solved by direct method	SIR92
Refinement on F	TEXSAN
R = 0.059 for 11586 with I > 1σ(I)	Δ/σ_{max} = 0.01
Rw = 0.060	$\Delta\rho_{max}$ = 0.44 e.Å^{-3}
S = 1.973	$\Delta\rho_{min}$ = -0.41 e.Å^{-3}

Refined parameters = 1909

$R = \Sigma \, ||Fo|-|Fc|| \, / \, \Sigma \, |Fo|$

$Rw = [\Sigma \, (\, |Fo|-|Fc| \,)^2/wFo^2]^{1/2}]$ with $w = 1 \, / \, [\sigma^2(Fo) + 3.4 \cdot 10^{-4} \, |Fo|^2]$

* solvate: $[5(CH_3OH) \cdot (CH_3CN) \cdot (CH_3CH_2OH)]$

Magnetic Susceptibility Studies.

Figure 2S: Temperature dependence of the product of the temperature and the molar susceptibility for **a(BPh$_4$)$_2$** at 0.5 T (Δ), 1 T (∇), 2.5 T (◊), and 5 T (O) magnetic field with the best least-squares fits (solid line).

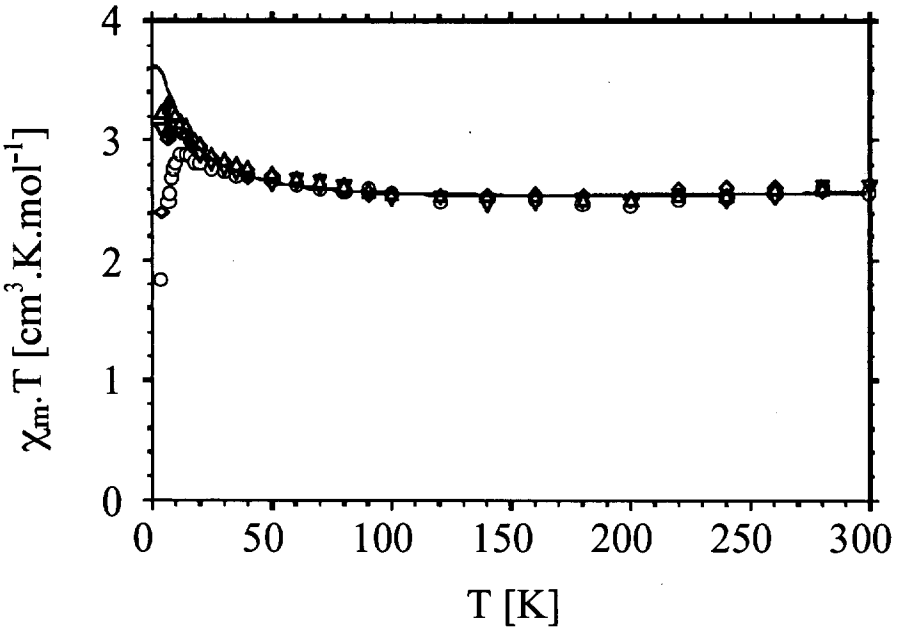

The best least-squares fit reproduced in this figure is obtained using the data at the four magnetic field together, in the valid temperature domain using the equations (1) and (2) proposed in the manuscript and led to the following values : J = 2.5(7) cm^{-1}, g = 2.19(6) and TIP = 200(200) × 10^{-6} cm^3.mol^{-1}. A fit with *TIP* fixed at 100 × 10^{-6} cm^3.mol^{-1} gave similar values : J = 2.2 cm^{-1} and g = 2.22.

NMR resonance assignment strategy.

Figure 3S: ^{1}H magnitude COSY spectrum (A) and downfield portion of the ^{1}H NMR spectrum (B) of **b**$(PF_6)_2$ in CD_2Cl_2 at 293 K. Data are acquired and processed identically to the COSY experiment presented in Figure 5 of the manuscript. Pyridyl and thiophenolic spin-systems are shown. Part (C) emphasizes the spin-system of the thiophenolic aromatic ring. Part (D) reproduces the ligand numbering scheme used for signal assignment.

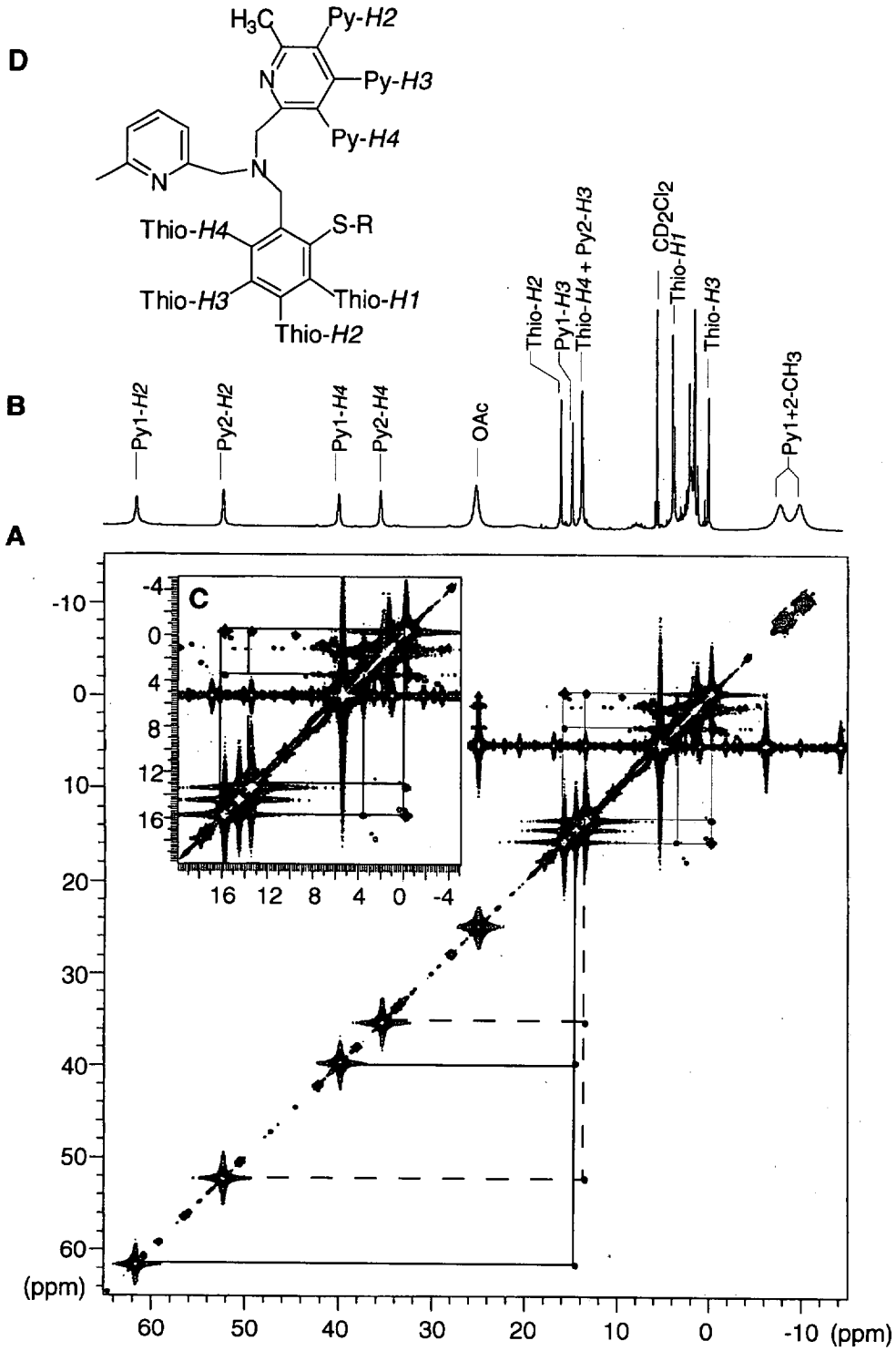

Figure 4S: Portions of the magnitude COSY spectrum for **c(PF$_6$)$_2$** in CD_2Cl_2 at 293 K, describing (A) the pyridyl aromatic spin-systems and (B) the thiophenolic spin-systems. Py1 and Py1' stand for the *H1* non-methylated pyridyl ring; Py2 and Py2' stand for the methylated pyridyl ring.

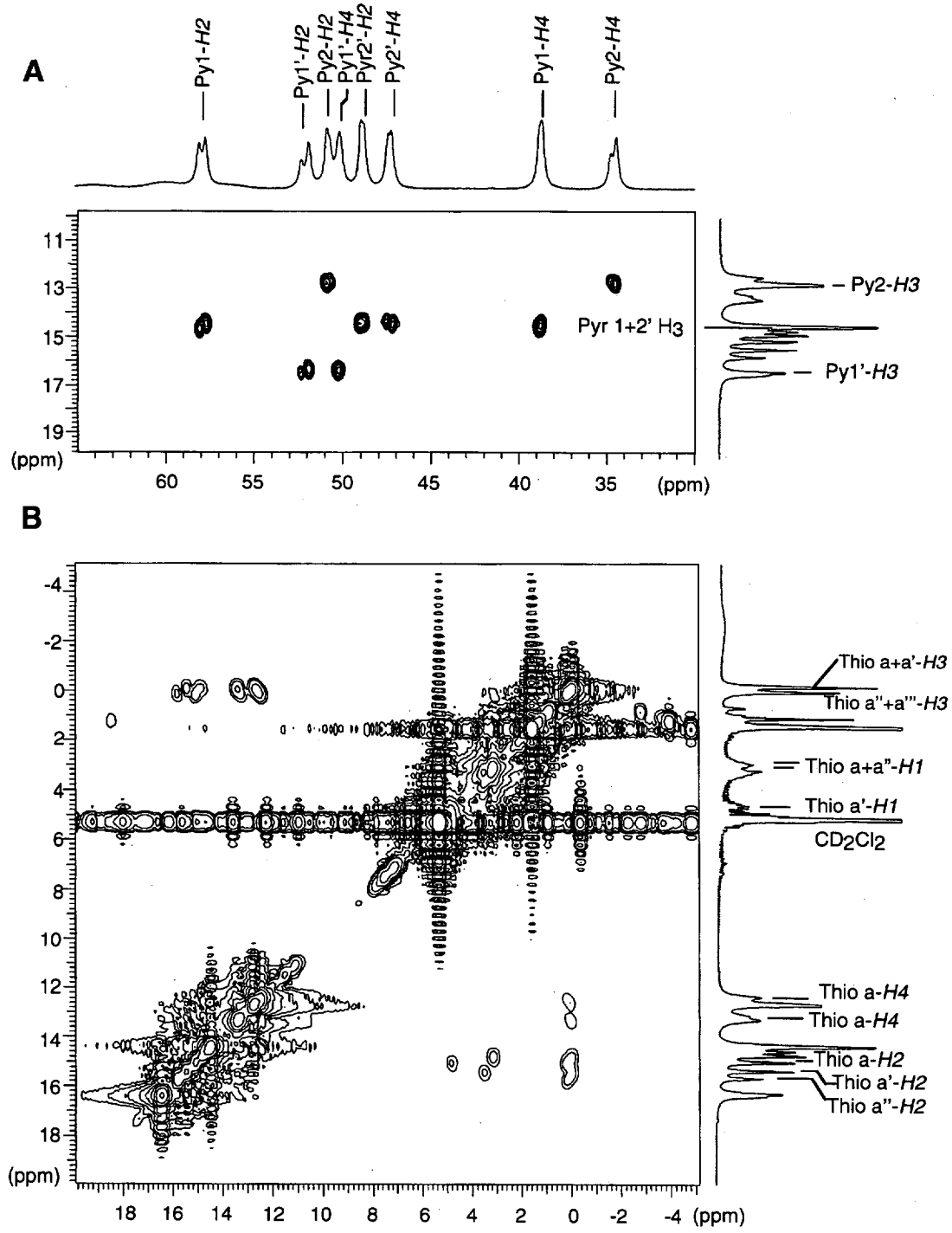

In each case, the pyridyl ring of interest can be in a *cis* or a *trans* position with respect to the thiophenolic groug anchoring the metal, thus leading to two inequivalent spin-systems labelled with and without a prime. Four thiophenolic ring spin-systems are observed due to *cis/trans* isomerism and are a signature for the presence of four stereoisomers in equal amounts in the mixture.

Table 2S: NMR parameters and resonance assignment for the two binuclear Ni^{II} complexes **a**$(PF_6)_2$ and **b**$(PF_6)_2$ in CD_2Cl_2 at 293 K. Results of chemical shift and relaxation rate temperature-dependence for complex **b**$(PF_6)_2$ in CD_2Cl_2.

Resonance assignment		Complex **a**$(PF_6)_2$ T= 293 K			Complex **b**$(PF_6)_2$ T=293 K			T dependence			T_1^{-1} slope[h]
		δ (ppm)[a]	T_1 (ms)[b]	T_2 (ms)[c]	δ (ppm)[a]	T_1 (ms)[b]	T_2 (ms)[c]	δ_{dia}[d] (ppm)	$a'\times$ 10^{-3}[d]	$b'\times$ 10^{-5}[d]	$\alpha\times10^{-3}$ ($ms^{-1}.K^2$)
Py1+2	*H1* or	155.43	0.26	0.1	-8.11	0.93	0.7	*2.51*	-3.2	-1.7	93.5(0.989)
	CH_3	171.43	0.24	0.2	-10.25	0.94	0.7	*2.51*	-2.8	-1.0	88.5(0.828)
Py1	**H2**	52.05	3.50	1.7	61.61	5.54	2.7	*7.38*	15.1	2.4	15.5(0.993)
	H3	16.42	8.57	6.4	14.46	14.30	8.8	*6.99*	2.2	0.5	6.0(0.985)
	H4	51.24	3.09	1.8	39.79	4.65	3.2	*7.23*	8.8	2.1	18.9(0.984)
Py2	**H2**	48.40	3.52	2.0	52.25	6.62	3.6	*7.38*	12.7	1.3	13.4(0.993)
	H3	14.27	9.04	7.0	13.43	13.30	5.6	*6.99*	1.9	-0.3	12.7(0.990)
	H4	48.40	3.52	2.0	35.27	4.84	3.4	*7.23*	7.5	2.2	17.9(0.996)
Thio	H_1	~ 5.32[e]			3.47	[e]	[e]	*7.31*	-3.1	4.1	[e]
	H2	15.36	11.74	8.4	15.72	18.72	11.0	*7.53*	2.2	0.5	4.7(0.996)
	H3	0.12	12.76	8.6	-0.28	19.71	11.0	*7.53*	-2.2	-0.2	4.4(0.999)
	H4	12.75	4.43	3.6	13.40	[e]	6.4	*7.53*	1.4	1.0	5.9(0.976)
CH_2H_{ea}	Py *trans*[f]	139.59	0.70	0.4	160.33	0.82	0.4	*3.79*	44.3	4.5	101(0.984)
	Py*cis*[g]	245.80	0.71	0.4	279.62	0.91	0.6	*3.79*	77.0	11.0	131(0.974)
	Thio	113.12	0.72	0.4	112.00	0.64	0.2	*3.88*	30.0	5.0	91.5(0.994)
CH_2H_{ax}	Py *trans*[f]	8.58	0.15	0.4	3.65						
	Py *cis*[g]	0.12			1.63						
	Thio	60.00	0.20	0.3	20.09	0.27	0.4	*3.88*	6.5	-5.2	
OAc	CH_3	25.87	1.30	1.0	24.92	1.60	1.4	*2.50*	6.5	0.5	51.0(0.833)

[a] Observed chemical shifts, in ppm, referenced to residual solvent resonance at 5.32 ppm.
[b] T_1 values obtained from the monoexponential fitting procedure of the inversion-recovery data on 36 array values. The error on these data is estimated to be less than 2.5%.
[c] T_2 values calculated from the linewidth measured on the 1D spectrum.
[d] Values obtained from a second-order polynomial fit of the Curie plot $\delta = f(1/T)$, where δ_{dia} (in ppm) is the diamagnetic observed shift for the free ligand, *a'* is the T^{-1} coefficient (in ppm.K) and *b'* is the T^{-2} coefficient (in $ppm.K^2$).
[e] Fortuitous overlap of resonances, that prevents relaxation times estimation.
[f] Methylene group bound to the pyridyl ring fixed to the metal in a *trans* configuration with respect to the thiophenolic group.
[g] Methylene group bound to the pyridyl ring fixed to the metal in a *cis* configuration with respect to the thiophenolic group.
[h] Values obtained from a fit of relaxation rate T_1^{-1} (ms^{-1}) *vs* the square of the reciprocal temperature (in K). Correlation coefficients are given within parentheses.

Table 3S: Resonance assignment, relaxation properties and temperature dependence of chemical shift values and relaxation rate, at 293 K, in the mixture of stereoisomers **c(PF$_6$)$_2$** in CD_2Cl_2.

Resonance assignment				Curie plot[c]		Polynomial plot[d]			T_1^{-1} slope[e]
		δ (ppm)[a]	T_1 (ms)[b]	δ_{int} (ppm)[c]	$a \times 10^{-3}$ [c]	δ_{dia} (ppm)[d]	$a' \times 10^{-3}$ [d]	$b' \times 10^{-5}$ [d]	$\alpha \times 10^{-3}$ [e] ($ms^{-1}.K^2$)
Py2+2'	***CH$_3$***	-9.14	0.91	*4.70*	-4.0	*2.53*	-3.0	-1.2	96.6(0.989)
		-9.80	0.88	*2.60*	-3.6	*2.53*	-3.6	0	99.3(0.993)
	CH$_3$	-11.18	0.88	*5.59*	-4.9	*2.53*	-3.4	-1.7	10.1(0.993)
		-12.12	0.84	*5.17*	-5.0	*2.53*	-3.5	-2.2	
Py1+1'	**H1**	160.71	0.53	*-10.85*	49.4	*8.51*	46.2	6.4	
	H1	174.59	0.30	*-2.79*	51.6	*8.51*	40.1	10.9	111.8(0.986)
Py1	**H2**	58.91	4.88	*3.91*	16.0	*7.34*	14.4	2.0	17.2(0.981)
		58.56	5.16	*4.25*	15.8	*7.34*	14.3	1.8	16.2(0.981)
	H3	14.61	13.29	*6.24*	2.4	*7.12*	2.0	0.5	6.4(0.999)
	H4	39.26	4.34	*4.15*	10.2	*7.21*	8.7	1.7	19.4(0.997)
Py2	**H2**	51.58	5.40	*6.32*	13.2	*7.34*	12.7	0.6	16.2(0.989)
	H3	12.90	11.01	*6.07*	2.0	*6.98*	1.5	0.5	8.0(0.919)
		12.86							
	H4	34.96	4.17	*4.73*	8.9	*7.21*	7.7	1.4	20.5(0.964)
		35.26	3.90	*3.99*	9.0		7.4	2.0	21.6(0.990)
Py1'	**H2**	53.04	4.45	*5.95*	13.7	*7.34*	13.0	0.8	19.1(0.994)
		52.64	4.82	*5.68*	13.7	*7.34*	12.8	1.0	17.6(0.997)
	H3	16.56	11.26	*6.82*	2.8	*7.12*	2.	0.2	7.5(0.994)
	H4	50.88	4.09	*5.51*	13.2	*7.21*	12.3	1.2	20.7(0.986)
Py2'	**H2**	49.63	5.44	*5.55*	12.8	*7.34*	12.0	1.0	15.7(0.999)
		49.53							
	H3	14.61	13.29	*6.24*	2.4	*6.98*	2.1	0.4	6.4(0.999)
	H4	48.10	4.36	*4.57*	12.8	*7.21*	11.4	1.5	19.3(0.993)
		47.92	4.52	*5.32*		*7.21*	11.4	1.5	
Thio	**H1**	3.43	3.11	*6.21*	-0.9	*7.56*	-0.7	0	25.0(0.874)
		3.10	3.42	*6.21*	-0.9	*7.56*	-0.7	0	24.3(0.874)
		4.80	3.45	*7.21*	-0.6	*7.56*	-1.4	0.7	25.4(0.955)
	H2	15.93	14.27	*6.76*	2.7	*7.56*	2.3	0.5	6.0(0.996)
		15.59	16.09	*6.87*	2.5	*7.56*	2.2	0.4	5.3(0.998)
		15.22	16.12	*6.81*	2.4	*7.56*	2.1	0.4	5.3(0.996)
		14.96	17.19	*6.94*	2.3	*7.56*	2.0	0.4	5.0(0.996)
	H3	0.05	17.1	*7.88*	-2.3	*7.56*	-2.2	-0.2	5.0(0.999)
		-0.18	18.35	*7.96*	-2.4	*7.56*	-2.1	-0.2	4.6(0.998)
	H4	13.33							
		13.49	6.05	*7.98*	1.6	*7.56*	1.8	-0.2	14.1(0.929)
		12.55	6.26	*7.46*	1.5	*7.56*	1.4	0.0	14.0(0.981)

Table 3S (continued):

Resonance assignment		δ (ppm)[a]	T_1 (ms)[b]	Curie plot[c] δ_{int} (ppm)[c]	Curie plot[c] $a \times 10^{-3}$ [c]	Polynomial plot[d] δ_{dia} (ppm)[d]	Polynomial plot[d] $a' \times 10^{-3}$ [d]	Polynomial plot[d] $b' \times 10^{-5}$ [d]	T_1^{-1} slope[e] $\alpha \times 10^{-3}$ [e] ($ms^{-1}.K^2$)
CH_2H_{eq}	Py1+1' *cis*	254.65	0.77	*-8.40*	7.7	*3.82*	70.6	7.2	272.8(0.952)
	Py2+2' *cis*	274.04	0.77	*-11.49*	83.0	*3.79*	75.6	9.1	10.8(0.864)
	Py1+1' *trans*	137.10 136.30	0.93	*0.68*	39.7				90.0(0.994)
	Py2+2' *trans*	159.09	0.53	*-10.86*	49.4	*3.79*	42.4	8.3	
	Thio	122.56	0.86	*-7.22*	37.9	*3.87*	32.6	6.2	97.7(0.985)
		108.24	0.96	*-8.58*	34.0	*3.87*	28.0	7.0	86.6(0.963)
CH_2H_{ax}	Thio	64.86	0.28	*8.45*	16.4	*3.87*	18.8	-3.0	
		60.59 57.50	0.34						
	Py *cis*	-2.92	0.49	*13.60*	-4.8	*13.06*	-4.5	-0.3	233.6(0.824)
OAc	CH_3	24.98	1.63	*1.70*	6.8	*2.50*	6.4	0.4	54.4(0.999)

[a] Chemical shifts, in ppm, referenced to residual solvent resonance at 5.32 ppm at 293 K. Py1+1' stands for the protonated pyridyl ring in *trans* or *cis* configuration with respect to the thiophenolic group. Py2+2' is used for the equivalent methylated pyridyl ring.

[b] T_1 values obtained from the monoexponential fitting procedure of the inversion-recovery data on 36 array values. A comparison of three independently acquired data sets yields to a maximal 2.5% error on the reported values.

[c] Fit of the chemical shift variations (in ppm) with temperature (in K), according to the Curie law:

$$\delta_{obs} = \delta_{int} + a/T$$

where δ_{int} is the intercept at infinite temperature and a is the Curie slope. Correlation coefficients are greater than 0.99 in each single case.

[d] Fit of the chemical shift variations (in ppm) with temperature (in K), according to a polynomial function:

$$\delta_{obs} = \delta_{dia} + a'/T + b'/T^2$$

where δ_{dia} is the observed diamagnetic shift in the ligand. Correlation coefficients are greater than 0.99 in each single case. $a' \times 10^{-3}$ (resp. $b' \times 10^{-5}$) is defined with a 0.2 ppm.K (resp. $ppm.K^2$) precision. They do not significantly differ from the values obtained in the case of the Curie law.

[e] Values obtained from a fit of relaxation rate T_1^{-1} (ms^{-1}) *vs* the square of the reciprocal temperature (in K). Correlation coefficients are given within parentheses.

Hyperfine shifts in nickel(II) dimers : Curie law deviations due to *D* and *J*.

Deviations to the usual Curie law can be understood considering the presence of one (or more) low-lying excited state(s), where the differences in energy between ground and excited levels are of the order of thermal energy k_BT. In the particular case of **a**$(BPh_4)_2$, each nickel center lays in a pseudo-octahedral environment of four different ligand atoms. The ligand field theory leads to a $^3A_{2g}$ orbitally nondegenerate ground state for each nickel atom and the spin levels may be split to a small extent through the zero-field splitting *D*, usually in the order of 0-60 cm^{-1} in mononuclear complexes. Such contribution also states for dinuclear species, although the magnitude of the zero-field splitting may differ from the mononuclear ones. According to Kurland and McGarvey (see reference 53), the contact hyperfine shift is then given by the following equation:

$$\delta_{hf} = -\frac{4g_e\beta_e K}{18\pi}\left[\frac{\chi_{xx}}{g_{xx}} + \frac{\chi_{yy}}{g_{yy}} + \frac{\chi_{zz}}{g_{zz}}\right] \quad (1)$$

where *K* is a constant which relates the orbital spin density contribution to the nuclear spin density and χ_{ii} are the principal axis components of the susceptibility tensor. In the case where electronic spin $S = 1$ is considered and where $D << k_BT$, the following expressions of the principal susceptibility components are obtained:

$$\chi_{zz} = \frac{2g_{zz}^2\beta^2\exp(-D/k_BT)}{k_BT[1+2\exp(-D/k_BT)]} = \frac{2g_{zz}^2\beta^2}{3k_BT}\left[1-\frac{D}{3k_BT}\right] \quad (2)$$

$$\text{and } \chi_{xx} = \chi_{yy} = \frac{2g_\perp^2\beta^2[1-\exp(-D/k_BT)]}{D[1+2\exp(-D/k_BT)]} \to 0 \quad (3)$$

This implies a T^{-1} but also additional T^{-2} temperature dependence of the hyperfine chemical shift.

In the dinuclear complexes studied, the two nickel atoms are furthermore ferromagnetically spin-coupled to each other and the resulting *J* coupling constant is an additional source to energy level splitting. If *J* is in the order of a few cm^{-1}, deviations to the Curie law can then occur. In a very elegant study by Shokheriev and Walker (see reference 54), the temperature dependence of hyperfine shifted signals for multilevel systems is described. By averaging the equations describing the hyperfine shift with their Boltzman weighting factors, the hyperfine shift δ_{hf} is given by:

$$\delta_{hf} = (1/Z)\sum\delta_{n,l}W_l\exp^{-E_l/k_BT} \quad (4)$$

where $\delta_{n,l}$ is the hyperfine shift of nucleus n in a pure electronic state l, E_l the energy of the considered level, W_l is the statistical weight of state l ($W_l = 2S_l + 1$) and *Z* is the statistical sum:

$$Z = \sum W_l\exp^{-E_l/k_BT} \quad (5)$$

For a three levels case, such as that found for high-spin nickel(II) dimers, where the $S' = 0$, 1 and 2 (S' is the total spin state) are significantly populated at room temperature and $E_l = -J[S'(S'+1)-S_1(S_1+1)-S_2(S_2+1)]$ (based on the hamiltonian $\hat{H} = -2J\hat{S}_1.\hat{S}_2$), equations 4 and 5 can be combined to equation 6 in the case where $J << k_BT$:

$$\delta_{hf} = \frac{1}{9T}\left(F_{n,0} + 3F_{n,1} + 5F_{n,2}\right) + \frac{J}{9k_BT^2}\left(-4F_{n,0} - 6F_{n,1} + 10F_{n,2}\right) \quad (6)$$

where $F_{n,0}$, $F_{n,1}$ and $F_{n,2}$ are the Curie factors of the $S' = 0$, $S' = 1$ and $S' = 2$ levels respectively. According to Shokheriev and Walker, a non-zero *J* coupling constant between the two nickel atoms ($J << k_BT$) then implies an additional contribution of $1/T^2$ to fitting expressions of the observed chemical shift.

Relaxation properties in $a(BPh_4)_2$: Temperature behavior.

Figure 5S: Observed relaxation rate *vs* reciprocal temperature for the resonance assigned to Py1-*H2* in the case of $\mathbf{a(BPh_4)_2}$ in CD_2Cl_2. The filled curve shows the result of a linear least-squares fit: Intercept = -0.38 ms^{-1}, slope = 204 $K.ms^{-1}$ and correlation coefficient = 0.993.

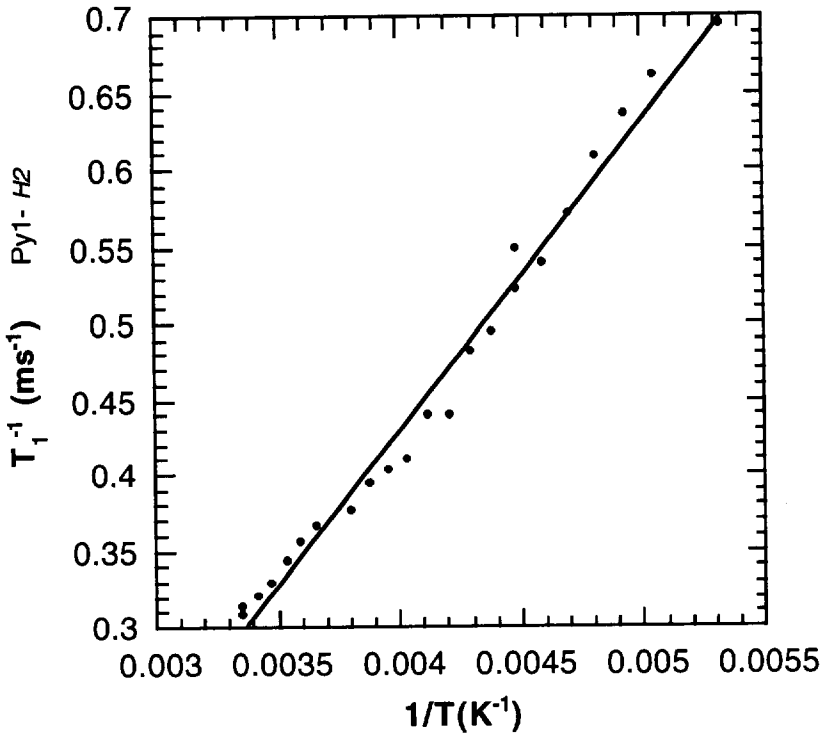

If the correlation coefficient is very similar to the polynomial fit (0.993 *vs* 0.995), the second order polynomial expression gives rise to more physically relevant data (see Figure 8 in the manuscript), especially with respect to the intercept value (positive value).